SAND2010-3276C

Passive Load Control for Large Wind Turbines

Thomas D. Ashwill[§]
Sandia National Laboratories[*], Albuquerque, New Mexico 87185

Abstract

Wind energy research activities at Sandia National Laboratories focus on developing large rotors that are lighter and more cost-effective than those designed with current technologies. Because gravity scales as the cube of the blade length, gravity loads become a constraining design factor for very large blades. Efforts to passively reduce turbulent loading has shown significant potential to reduce blade weight and capture more energy. Research in passive load reduction for wind turbines began at Sandia in the late 1990's and has moved from analytical studies to blade applications. This paper discusses the test results of two Sandia prototype research blades that incorporate load reduction techniques. The TX-100 is a 9-m long blade that induces bend-twist coupling with the use of off-axis carbon in the skin. The STAR blade is a 27-m long blade that induces bend-twist coupling by sweeping the blade in a geometric fashion.

I. Introduction

The Wind Energy Department at Sandia National Laboratories (SNL) conducts research in several technology areas that provide innovations for large wind turbine rotors and blades. Innovations are targeted at lowering the cost-of-energy and developing increasingly more efficient rotors that are lighter, more reliable and able to capture additional energy. These goals can be met through a variety of technologies: advanced materials, designs that optimize both aerodynamic and structural performance, and load alleviation [1]. Passive load control is the subject of this paper as Sandia has been working in this area for over a decade now. Lowering loads to the blade in a passive manner (primarily in Region III) leads to either lighter blades or longer blades for the same turbine power rating. Lighter blades help reduce the rate of increase of gravity loads that come with the trend to go to larger and larger turbines. Longer blades for the same rating effectively "moves the power curve to the left" resulting in increased energy capture. The incorporation of bend-twist coupling into blades is the concept used to create the passive load control. The bend-twist coupling concept allows for more twist as the blade bends, which lowers the angle of attack and reduces loads; performance is maintained by adjusting the pitch schedule. This paper will review the SNL work that created the bend-twist coupling theory and discuss the test results of two prototype blades that incorporate coupling in two distinct ways. The TX-100, a 9-m long blade, uses off-axis materials, and the K&C STAR 27-m blade uses geometric sweep to create this coupling for reduction of loads in a passive manner.

II. Passive Load Control

Previous work has shown the potential for modifying blade designs to incorporate bend-twist coupling in ways that passively reduce loads in high winds [2-7]. For passive load control using bend-twist coupling, blades can be designed in a least two different ways. Geometric-based coupling uses sweep along the blade to create a moment that induces twist [8]. A second method, material-based coupling, aligns the primary load-carrying spanwise fibers in an off-axis manner by about 20 degrees, so as the blade bends, it twists more than normal allowing loads to be relieved. In both cases, the idea is to effectively create more coupling between the flap and twist motions of the blade. Necessary design goals are to maintain flapwise strength and maximum tip deflection.

> Bend-twist coupling in wind turbine blades can reduce both fatigue and extreme operating loads, especially when applied in conjunction with a pitch-controlled rotor. This type of coupling has

[§] Technical Staff, Wind Energy Dept., MS1124, Senior Member AIAA
[*] Sandia is a multiprogram laboratory operated by Sandia Corporation, a Lockheed Martin Company for the United States Department of Energy's National Nuclear Security Administration under contract DE-AC04-94AL85000.

been used in other industries, implemented either through biased composite lay-ups or with the use of swept wings. Bend-twist coupling allows a turbine blade to twist while bending under load, lowering the effective angle of attack, and reducing aerodynamic loading. This is most effective in Region III where high winds cause significant fatigue damage and power can be maintained with adjusting the pitch angle. Critical issues for implementation into wind turbine blades lie in the detailed design and manufacturing of such bend-twist coupled blades. Due to their anisotropic mechanical properties, fiber reinforced plastics allow the designer to vary the stiffness in different loading directions to develop what are called bend-twist coupling effects. As detailed in Ref. 6, coupling levels are defined by a parameter, alpha, that indicates the proportion of the theoretically possible coupling. The coupling terms are generated starting with beam stress-strain relations. For bending twist-coupling the “stress-strain” relations at a point along the blade span, *x*, are given by:

$$\begin{bmatrix} EI & -g \\ -g & GK \end{bmatrix} \begin{bmatrix} \dfrac{\partial \theta}{\partial x} \\ \dfrac{\partial \varphi}{\partial x} \end{bmatrix} = \begin{bmatrix} M_b \\ M_t \end{bmatrix} \qquad (1)$$

Here, $\theta = \partial v/\partial x$ is the flapwise slope of the blade (v is the flapwise displacement), M_b is the flapwise bending moment, φ is the blade twist, and M_t is the twisting moment. The quantities EI and GK are the flexural rigidity and torsional stiffness respectively, and g is the coupling term which has a value of zero for the standard beam where no coupling is present. For this system to be positive definite, g is taken to be:

$$g = \alpha\sqrt{EIGK}\ , \quad -1 < \alpha < 1 \qquad (2)$$

The coupling coefficient, α, provides for variable coupling within the designated limits. Practical experience suggests that α may be limited to $-0.6 < \alpha < 0.6$ for material-based coupling. For geometric-based coupling, the coupling term, g, can be zero. It has been shown through aeroelastic modeling and analysis that loads can be reduced significantly with the use of bend-twist coupled blades while keeping the energy production the same and maintaining static and dynamic stability [6].

Early studies (1999-2000) examined the lay-up orientations required to gain improved bend-twist coupling and the extra benefits of adding carbon fibers to the material composition. Ong and Tsai [9, 10] note that the three key parameters that have the greatest effect on bend-twist coupling are the ply orientation, laminate material, and proportional volume of anistropy layers in a laminate. They determined that the optimum angle at which to place the biased fibers is 20 degrees and indicate that a 50% higher coupling coefficient can be obtained using carbon fibers in place of traditional glass fibers. They also placed a practical limit on alpha of less than 0.6 for airfoil shapes with closed cell cross-sections, although even this level may be difficult to attain due to conflicting constraints. De Goeij, Van Tooren, and Beukers [11] document similar work.

A series of concepts studies were performed for Sandia in 2002 that developed detailed methods for implementing such ideas into blades [7]. Three studies have examined decidely different approaches. 1.) The GEC effort [7, 12] developed conceptual designs based on a traditional structure consisting of two skins, two webs, and built-up spar caps. Three different geometries were modeled with the use of biased carbon fibers: spar cap only, skin only and both skin and spar cap. Significant coupling was obtained, but the cost estimates indicate an increase of at least 34% over the baseline. 2.) Wichita State [7, 13] studied the feasilibility of using braided composite preforms to manufacture a blade. Different arrangements of continuous structural boxes were modeled to determine levels of coupling that could be achieved. It was shown that braided composite blade can be manufactured with the desired stiffness and coupling properties. 3.) MDZ Consulting [7, 8] took a different approach by studying the possibility of inducing twist through the use of a curved planform (distributed sweep) and carbon fiber spar caps (with conventional fiber orientations).

III. TX-100 Blade

In 2002 SNL initiated a research program [14, 15] to demonstrate the use of carbon fiber in subscale blades and investigate innovative concepts through the WindPACT Blade System Design Studies (BSDS) via design studies and prototype fabrications [16, 17, 18]. Three 9-m designs were created with assistance from Global Energy Systems Consulting (GEC), Dynamic Design Engineering, and MDZ Consulting; and seven blades from each design were manufactured by TPI Composites. All blades were designed for a 100 kW stall controlled turbine. The first blade set was called CX-100 (Carbon Experimental), and contained a full-length carbon spar cap, a relatively new concept at the time. The geometry of the CX-100 is based on the design of the ERS-100 [19] blade at outboard span stations, and the Northern Power Systems NW-100 blade in the root area.

The second blade design, the TX-100 (Twist-Bend Experimental), has the same geometry as the CX-100, but was designed to have passive load reduction by orienting unidirectional carbon 20° off of the pitch axis in the skins from approximately 25% span outward. The TX-100 also contained a fiberglass spar cap which terminated at the mid-span of the blade.

The third blade design, termed the BSDS Blade, includes features as a thin-walled, large-diameter root; flatback airfoils; integrated root studs; and a full-length, constant-thickness, carbon spar cap. The BSDS blade does not include any load reduction and will not be discussed here (See Ref. 16 for further information).

A drawing of these blades is shown in Fig. 1 with the carbon areas shown in blue. Note the carbon spar caps of the CX-100 and BSDS blades, and the carbon in outboard skins of the TX-100. The unidirectional fiberglass spar cap of the TX-100 is shown in red and extends only to the mid-span of the blade. It was determined that the large amount of carbon contained in the skin was adequate to carry loads outboard in this design, making a full length spar cap unnecessary. The CX-100 is the baseline for the TX-100 testing.

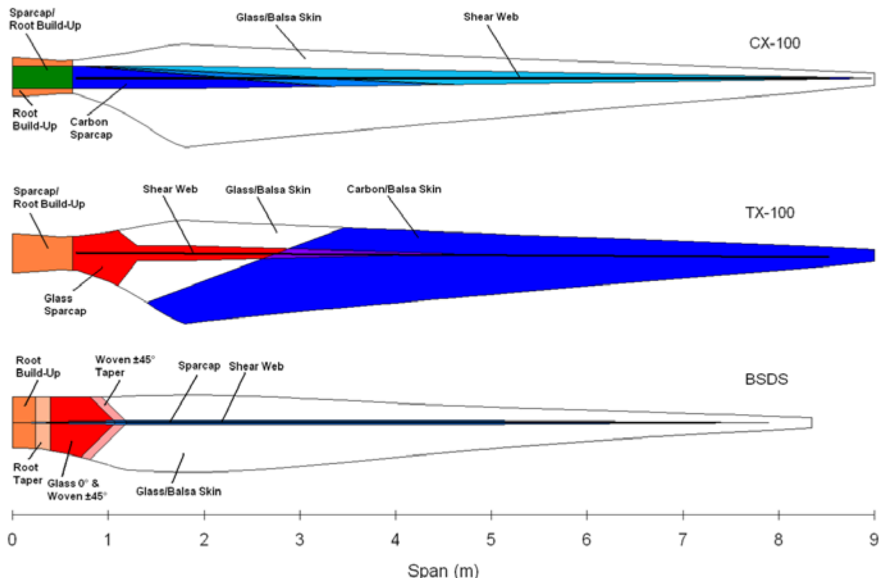

Figure 1. 9 m blade planform & material locations.

Under static testing, both CX-100 and TX-100 test blades survived factored design loading (Table 1). The CX-100 blade displayed exceptional stiffness, deflecting only 1.05 m at a root moment of 128.6 kN-m. The blade failed due to panel buckling near max-chord which was likely initiated by a separation between the shear web and low-pressure skin in that region. The TX-100 blade failed at a higher % above design load (slightly lower magnitude) than the CX-100 blade and in a similar location. The TX-100 blade successfully demonstrated twist-bend coupling caused by 20° off-axis carbon in the outboard skins as seen in Fig. 2, which compares predicted and measured twist distribution along the blade.

Table 1: Summary of results of 9-m blade static tests.

Property	CX-100	TX-100
Weight (lb)	383	361
% of Design Load at Failure	115%	197%
Root Failure Moment (kN-m)	128.6	121.4
Max. Carbon Tensile Strain at Failure (%)	0.31%	0.59%
Max. Carbon Compressive Strain at Failure (%)	0.30%	0.73%
Maximum Tip Displacement (m)	1.05	1.80

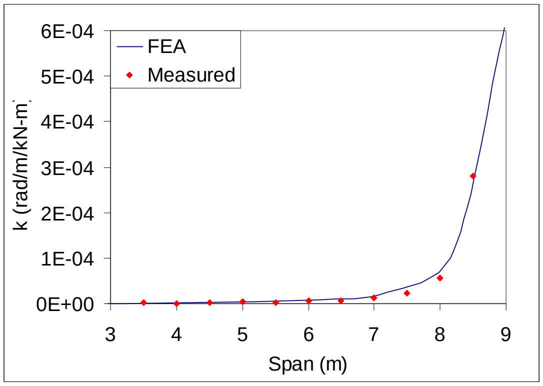

Figure 2. Twist distribution of TX-100: measured and predicted.

Figure 3. Fatigue testing of TX-100 blade at NREL's NWTC.

The CX-100 and TX-100 blades were also successfully tested to the 20-year equivalent fatigue test loads (Fig. 3).

Field testing of the CX-100 and TX-100 occurred in the 2007-08 time frame at the USDA site in Bushland, TX on a heavily instrumented Micon 65 turbine [20], which is fixed-speed and fixed-pitch. The measured power production of the CX-100 and TX-100 blade sets is shown in Fig. 4. The results are plotted as bin averages and include both the average power and the average of the maximum and minimum power outputs. The TX-100 power production is slightly lower than that of the CX-100. This is due to the blades sharing the same molds and thus the same pre-twist distribution. When loaded, the TX-100 blade no longer has an optimal twist distribution, which can be corrected for in a new design without pre-existing constraints.

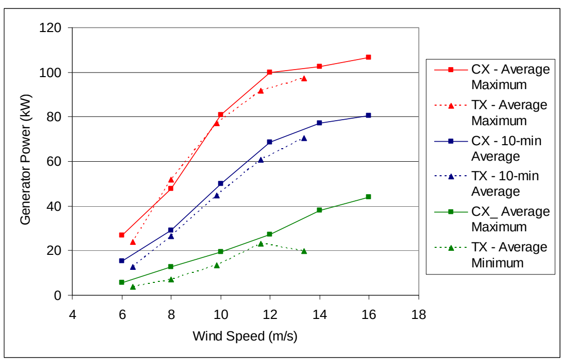

Figure 4. CX-100 and TX-100 measured power production.

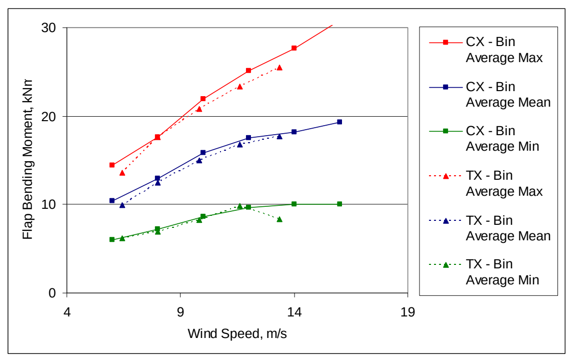

Figure 5. CX-100 and TX-100 measured root flap moments.

Measured root flap moments as a function of wind speed for the CX-100 and TX-100 are shown in Fig. 5. The TX-100 can be seen to have lower loads for all three averaged conditions: mean, minimum and maximum.

Files from CX-100 and TX-100 tests with nearly identical mean wind speeds and turbulence intensities were selected for direct comparisons (see Table 2). The results of the blade-root, flap-moment azimuth averages are shown in Fig. 6 as a percentage of the average root flap moment. The reduced load variability of the TX-100 blade is evident at all wind speeds.

File #	Mean Wind Vel. (m/s)		Turb. Intensity (%)	
	CX	TX	CX	TX
1	8.0	8.00	7.4%	7.6%
2	10.0	10.0	9.4%	11.5%
3	12.1	11.7	11.0%	12.9%

Table 2. Mean wind velocity and turbulence intensity for azimuth average files.

Root flap moment fatigue cycle counts from both blade tests were also compiled. The results for the 7-9, 9-11, and 11-13 m/s wind speed bins are shown in Fig. 7. The TX-100 blade has a reduction of high load cycles that become more pronounced as wind speeds increase. Paquette [20] performed a linear Miner's rule damage summation assuming a fatigue slope exponent of 10 on the rainflow cycle counts, and the results are shown in terms of the reductions in both fatigue damage rate and fatigue damage equivalent load in Table 3. Here it can be observed that it is possible to achieve as much as a 24% reduction in damage equivalent load in the 11-13 m/s wind speed bin.

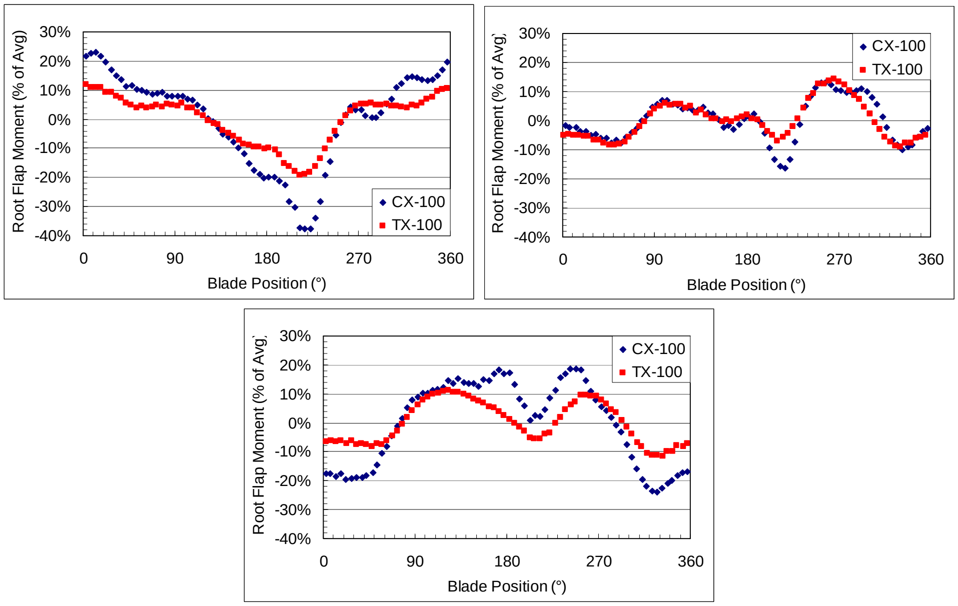

Figure 6. Azimuth averaged measured root flap moments as a percent of the average moment for CX-100 and TX-100 blades at 8 m/s (upper left), 10 m/s (upper right), and 12 m/s (bottom).

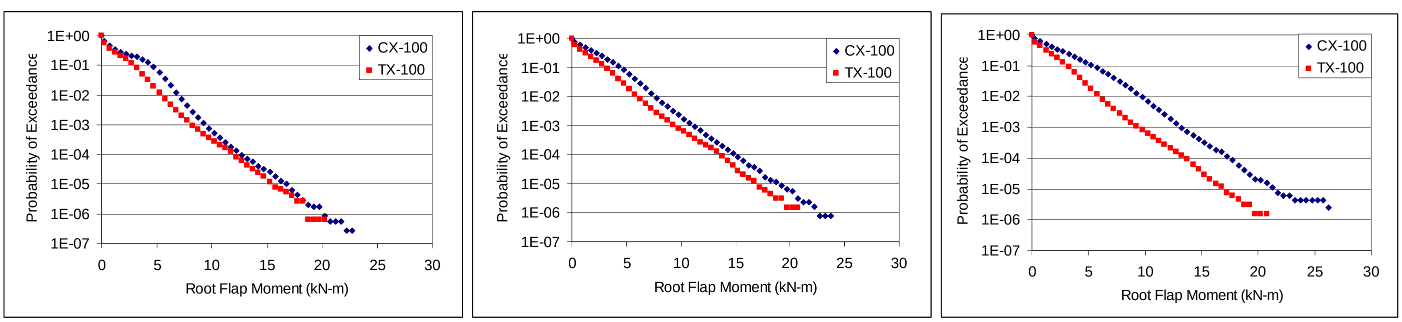

Figure 7. Root flap moment cycle counts for CX-100 and TX-100 blades at 7-9 (left), 9-11 (middle), and 11-13 (right) m/s wind speeds.

Wind Speed (m/s)	Relative Damage Rate (%)	Relative Damage Equivalent Load (%)
7-9	-53.8%	-7.4%
9-11	-69.1%	-11.1%
11-13	-93.6%	-24.0%

Table 3. Relative root flap fatigue damage rate and damage equivalent load for TX-100 compared to CX-100.

IV. Knight & Carver Sweep-Twist Blade

In late 2004, Knight & Carver (K&C) was contracted by Sandia National Laboratories (SNL) to develop a sweep-twist adaptive blade to passively reduce operating loads and allow for a larger, more productive rotor. As noted earlier, the feasibility of using geometric sweep to reduce fatigue loads had been established in previous work at SNL [7, 8]. Reduced fatigue loads would allow for a longer blade for the same fatigue spectrum; thus the rotor swept area grows and more energy is captured. After design and fabrication of the Sweep-Twist Adaptive Rotor (STAR) blade, laboratory testing (static, fatigue and modal) was successfully completed. Full flight testing recently has verified the predicted performance and operating loads [21, 22]. As will be discussed in the rest of this section, the STAR blade exceeded the primary project goal of improving annual energy capture over the baseline by 5-8% while keeping critical loads at the same levels.

A. Parametric Studies and Design of STAR Blade

The STAR blade project began in the fourth quarter of 2004 and proceeded in several stages. The first year was a design phase used to complete parametric and concept studies, preliminary designs and analyses, and a final design. After the first prototype blade was fabricated and statically tested early in 2006, a few modifications to the blade design were implemented. The field and fatigue test blades were fabricated in the fall of 2007. The blades were installed on the test turbine in Tehachapi, California during the winter of 2008. Field testing began in April 2008 and was completed that summer. Fatigue testing at NREL started in the summer of 2008 and was completed early in 2009.

The design phase began with a series of parametric and concept studies performed to determine the best options of manufacturing process and composite materials to use for this project. The Zond 750 was chosen as the baseline turbine; the Z-50 rotor blades are 24.5 m long, Z-48 rotor blades are 23.5 m long. Concept studies considered variation on degrees of sweep and airfoil composition to determine the most desirable combinations. (Figs. 8, 9]

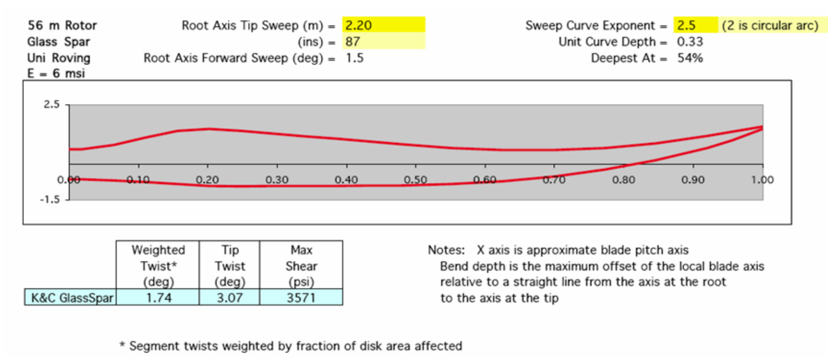

Figure 8. Concept design.

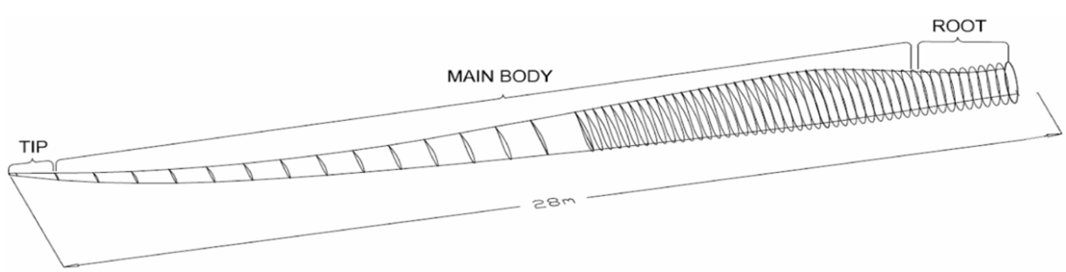

Figure 9. Design planform and airfoil stations.

This design was complicated by the fact that the STAR blade is a retrofit to an existing machine. This meant that the design was constrained to the operation window of the Z-750 baseline. Parameters for optimization of sweep and blade length included: planform, airfoil properties, sweep magnitude and curve, spar cap position and sizing, materials and manufacturing process, and root forward sweep. Other parameters, such as total sweep, RPM, blade stiffness, mass, and CG, were either fixed or somewhat limited. Full system analytical calculations were performed using FAST and ADAMS; detailed stress analyses including buckling estimations were performed using ABACUS.

The final configuration met the major design requirements as shown:

	Target	STAR Design
• Axis mass moment (kg-m)	19,661	20,000
• Deflection at Max Power	56.6”	56”
• Flatwise frequency	3.75p	> 3p
• Edgewise frequency	4.57p	> 4p
• Flatwise loads	Similar to existing	
• Pitch moment	Similar to existing	
• Materials	Fiberglass	Fiberglass

Figure 10 shows the final design drawings of a typical cross-section of the blade.

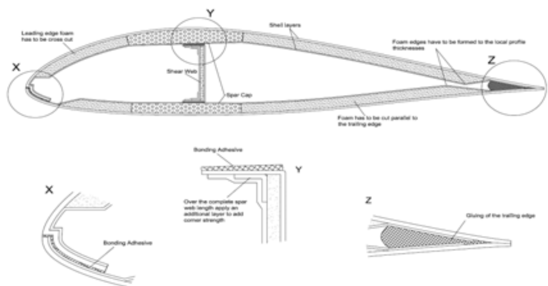

Figure 10. Cross-Section of blade outboard.

Figure 11 shows results from full system loads analyses. For both PSD’s of root moment and pitch moment (not shown – see Ref. 21), a similar pattern is observed. Adding 10% length to the baseline with no sweep grows the loads significantly. Adding sweep reduces the loads back to similar values as the original baseline. The bottom line is that the increased length implemented in the STAR blade (27.1 m) was predicted, as hoped for, to have the same load distribution as the smaller straight baseline at 24.5 m.

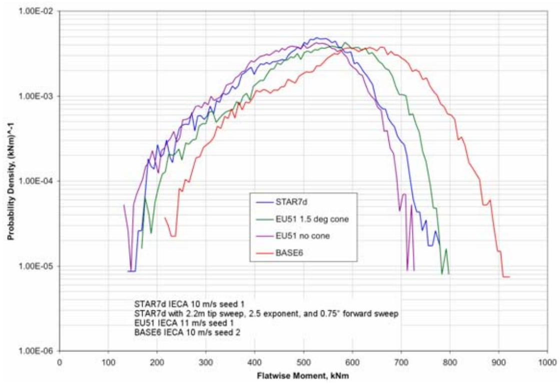

Figure 11. Flatwise root moment.

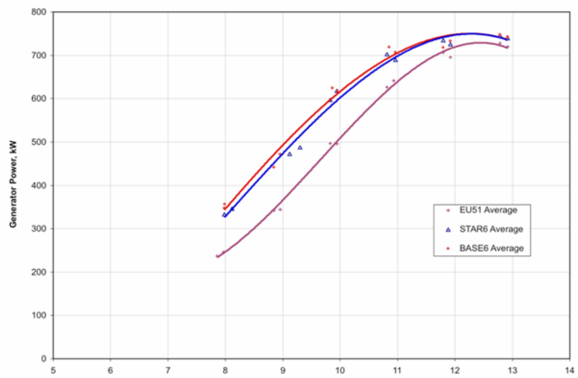

Figure 12. Baseline vs. STAR (est.) generator power.

The STAR power curve, Fig. 12, shows the amount of increased power that is predicted for winds below rated.

B. Fabrication and Testing of STAR Blade

After fabrication (Fig. 13), the first blade was tested statically at K&C facilities at three load levels – 50% and 100% of maximum operating load and proof load. Figure 14 shows the static test arrangements including the barrel-type loading configuration.

Figure 13. Fabrication of first STAR blade.

Figure 14. Static testing of first STAR blade.

Figure 15. STAR blades mounted for flight testing.

After a few design modifications made based on static test results, four STAR blades were built. One blade was tested to its 20 year equivalent fatigue load at NREL's NWTC in Boulder, CO. The other three blades have been undergoing flight testing for several months. Figure 15 shows the STAR blades being mounted on the Zond turbine.

C. Field Testing

The primary goal of field testing was to measure blade loads for the STAR rotor and compare them to the representative loads for the turbine. A secondary goal was to compare the performance of the STAR rotor to reference turbines operating under similar conditions.

The field test turbine was a Zond 750 (Z-48) turbine which operates at a rated speed of 34.4 rpm and originally had a 48 meter rotor with 23.5 m long straight blades. The STAR field testing used a two channel sensor system, which has proven to be successful on prior projects. Strain gages were used to measure blade root bending moments on the Z48 turbine equipped with the longer STAR prototype blades (26.1 m) and a 54 meter diameter rotor. The field test team, led by Kevin Jackson of Dynamic Design, had previously used a similar approach to measure data on Zond 750 kW turbines with conventional blades at two sites in Iowa and Minnesota. This approach provided a broad comparison of actual operating loads between the STAR rotor and other Z750 turbines in a range of configurations and environments (Figs. 16, 17).

The test site is located in the Tehachapi Mountain wind resource area of California. The test turbine is located within an existing wind plant several miles southeast of the town of Tehachapi, California. The elevation of the test site is approximately 4920 feet and the hub height is slightly more than 5000 feet above sea level. Wind conditions at the site are within the IEC Class II designation.

Field test data were initially collected using natural wind excitation with the turbine not operating. These data were used to determine the natural frequencies of the STAR blade when installed on the test turbine. Results were that the non-rotating frequency of the first blade flatwise mode (1.83 Hz) was slightly lower than the predicted value (1.98 Hz), while the measured blade edgewise frequency (2.6 Hz) was somewhat higher than the calculated value (2.43 Hz). The measured system natural frequencies were well placed between operating harmonics and dynamic amplification through resonance was ruled out as a concern prior to operation of the turbine.

Comparisons between measured loads for the STAR 54 rotor (Tehachipi site) and Zond Z-48 rotor (Iowa and Minnesota sites) are presented in Figs. 16 and 17. A conventional 54 meter diameter rotor would have increased blade root bending moment by 80% as compared to the baseline. These results show that measured blade root bending moments for the STAR 54 rotor are comparable to loads measured on the baseline Z-48 and no significant increase in loading occurred. The STAR rotor operated in the field as expected and successfully sheds high blade root bending loads through passive bend-twist coupling.

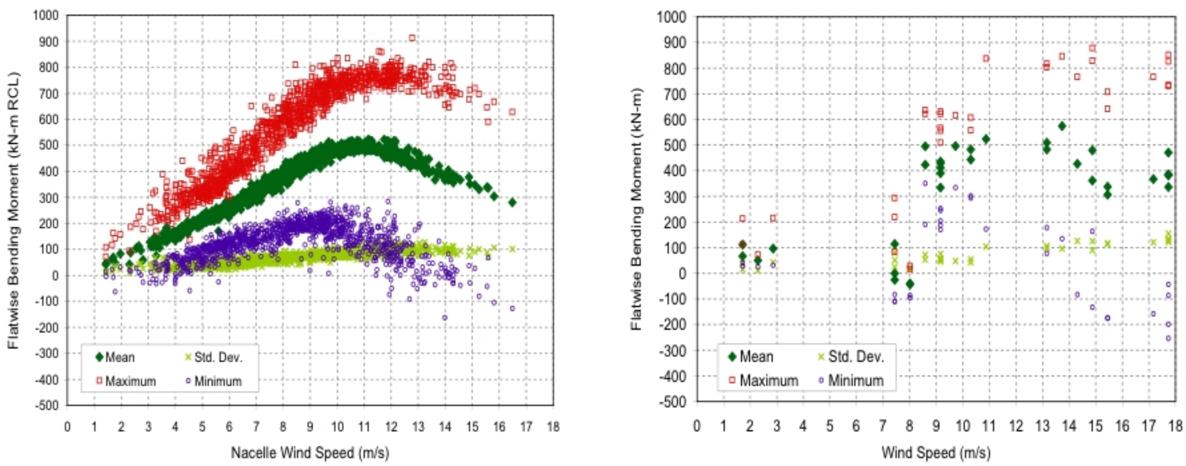

Figure 16. Measured flatwise bending moments – STAR 54 (left) and baseline Z48 (right).

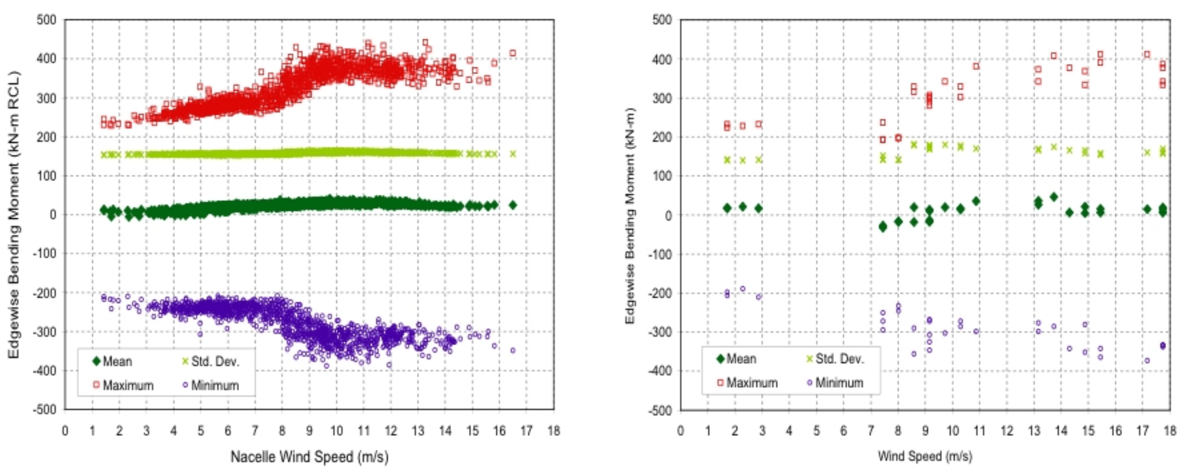

Figure 17. Measured edgewise bending moments – STAR 54 (left) and baseline Z48 (right).

Sets of power curves for Group 1 and 2 turbines are shown in Fig. 18 (Group 1 turbines sit next to the STAR turbine on a ridgeline; Group 2 turbines are located at a slightly lower elevation upwind of the STAR turbine and appear to have lower average wind speeds and turbulence). Figure 19 compares power curves for the STAR 54 and the best of the low turbulence Tehachipi turbines (Group 2) to their respective models, showing good results. Data for the STAR 54 rotor are somewhat less well correlated to the 54-m model than Group 2 is to the 48-m model as a result of the relatively high wind speed and turbulence of the STAR 54 test turbine site.

The sorted data were used to calculate the average energy capture for each of the groups over the online period, which is summarized in Table 1. Group 1 consisted of 3322 10 minute data points, when all five Group 1 Tehachipi turbines were simultaneously producing power. The group analysis shows that energy capture for the STAR rotor was approximately 12% better than the Group 1 turbines and about 36% better than the Group 2 machines.

Measured moments at the blade root were compared to predictions from the ADAMS model for the STAR 54 rotor operating on a Z-48 turbine. The air density in the ADAMS model assumed an elevation of 5000 feet above sea level, which matched the turbine site altitude. The predicted flatwise moments were in good agreement with the ADAMS model predictions. *Maximum* flatwise moments were somewhat lower than those calculated by the ADAMS model, which is a positive aspect (Fig. 20). *Mean* flatwise loads compared very closely to predictions [21, 22].

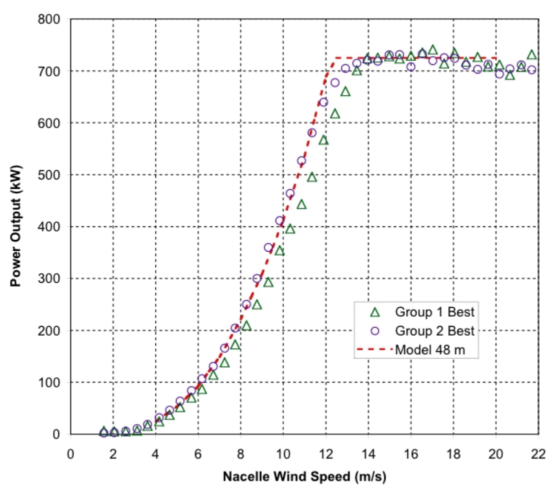

Figure 18. Best of group 1 and group 2 power output compared to 48-m models.

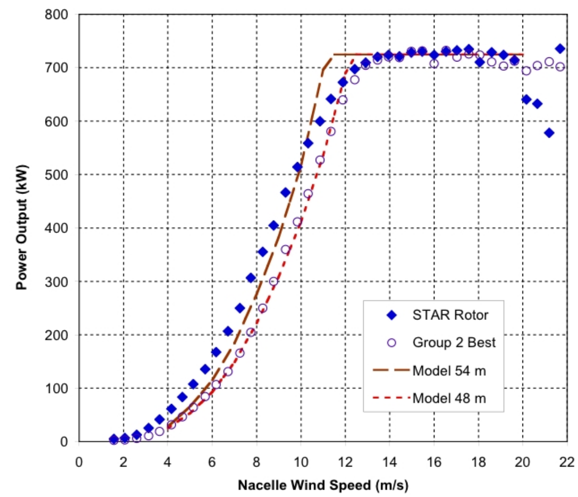

Figure 19. STAR and best of group 2 power output compared to 54-m and 48-m models.

Turbine Group 1	Energy (kWh)	Compare
RP-01	243009	101%
RP-02	236301	99%
RP-04	237148	99%
RP-08	242496	101%
Average	239738	100%
STAR	268711	112%

Table 4. Comparison in energy capture for Group 1 turbines.

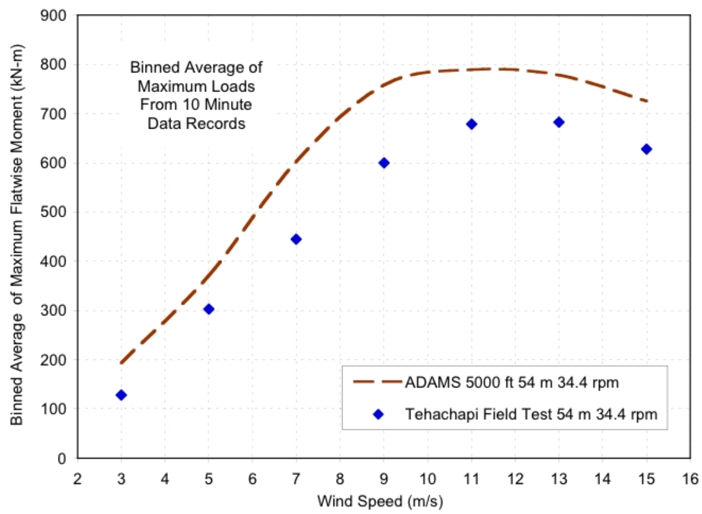

Figure 20. Comparison of measured binned average flatwise moments to ADAMS model.

SUMMARY

Passive bend-twist coupling has been demonstrated in two wind turbine prototype research blades and shows very good potential in lowering the cost-of-energy of large wind turbines.

The 9-m TX-100 blade incorporates bend-twist coupling with off-axis carbon in the blade skin. The blade has been fully tested and shown enhanced strength compared to a carbon-spar blade with no bend-twist coupling. The test results also confirmed that using off-axis carbon in the skin will induce extra twist and alleviate loads. The full benefits of this design can be realized with an ideal pre-twist design for a larger, utility grade size turbine.

The 27-m STAR blade incorporates bend-twist coupling using geometric sweep. Static, fatigue, and resonance tests were completed. Flight testing has confirmed that for an increase of 10% in blade length with sweep, the annual energy capture can be increased by 12%. Operational measurements confirm analytical predictions that the loads remain the same as the smaller straight-bladed baseline. Load reduction amounts may be enhanced with the optimization of sweep and blade length for a new design without operational window constraints.

ACKNOWLEDGEMENTS

The Sandia Labs/USDA test team provided the testing for the TX-100 and CX-100 blades, including data collection, post-processing and analysis. This team includes: Josh Paquette, SNL-Team Lead; Wesley Johnson, SNL; Byron Neal, USDA; and Adam Holman, USDA.

The Knight & Carver (K&C) team that designed, fabricated and tested the STAR blade consists of many people. Gary Kanaby, K&C, is the project lead. Key members for field testing are Kevin Jackson, Dynamic Design; Mike Zuteck, MDZ Consulting; Eric Jacobson, Jacobson Technical Services; and the Terra Gen Power crew.

REFERENCES

1. Ashwill, T.D., “Materials and Innovations for Large Blade Structures: Research Opportunities in Wind Energy Technology,” AIAA-2009-2407, *50th AIAA Structures, Structural Dynamics, & Materials Conference*, Palm Springs, CA, May 2009.
2. Veers, P.S. Bir, G. and Lobitz, D.W. "Aeroelastic Tailoring in Wind-Turbine Blade Applications," *Proceedings, Windpower '98 Meeting*.
3. Lobitz, D. and Veers, P., “Aeroelastic Behavior of Twist-coupled HAWT Blades,” *Proceedings, ASME/AIAA Wind Energy Symposium*, Reno, NV, 1998.
4. Lobitz, D. and Laino, D., “Load Mitigation with Twist-coupled HAWT Blades,” *Proceedings, ASME/AIAA Wind Energy Symposium*, Reno, NV, 1999.
5. Lobitz, D.W., Veers, P.S. and Laino, D.J. “Performance of Twist-Coupled Blades on Variable Speed Rotors,” *Proceedings, ASME/AIAA Wind Energy Symposium*, Reno, NV, 2000.
6. Lobitz, D. W., Veers, P.S., Eisler, G.R., Laino, D. J., Migliore, P.G. and Bir, G., “The Use of Twist-Coupled Blades to Enhance the Performance of Horizontal Axis Wind Turbines,” SAND2001-1003, Sandia National Laboratories, Albuquerque, NM, May 2001.
7. Ashwill, T.D., Veers, P.S., Griffin, D., Locke, J., Contreras, I., Zuteck, M.D., “Concepts for Adaptive Wind Turbine Blades,” AIAA-2002-28, *Proceeding, ASME/AIAA Wind Energy Symposium*, Reno, NV, 2002.
8. Zuteck, M.D., “Adaptive Blade Concept Assessment: Curved Planform Induced Twist Investigation," SAND02-2996, Albuquerque, NM, 2002.
9. Ong, C. H. and Tsai, S.W., “Design, Manufacture and Testing of a Bend-Twist D-Spar,” SAND99-1324, Sandia National Laboratories, Albuquerque, NM, June 1999.
10. Ong, C-H. and Tsai, S.W., “The Use of Carbon Fibers in Wind Turbine Blade Design,” SAND2000-0478, Sandia National Laboratories, Albuquerque, NM, March 2000.
11. de Goeij, W. C., van Tooren, M.J.L. and Beukers, A., “Implementation of Bending-Torsion Coupling in the Design of a Wind-Turbine Rotor-Blade,” Applied Energy, Vol. 63, 1999.
12. Griffin, D.A., "Evaluation of Design Concepts For Adaptive Wind Turbine Blades," SAND02-2424, Sandia National Laboratories, Albuquerque, 2002.
13. Locke, J. and Hildago, I.C., "The Implementation Of Braided Composite Materials In The Design Of A Bend-Twist Coupled Blade," SAND02-2425, Sandia National Laboratories, Albuquerque, 2002.
14. Ashwill, T.D., “Developments in Large Blades for Lower Cost Wind Turbines”, *Proceeding, AWEA 2004*, Chicago, Illinois.
15. Ashwill, T.D., and Laird, D., “Concepts to Facilitate Very Large Blades,” AIAA-2007-817, *Proceedings, ASME/AIAA Wind Energy Symposium*, Reno, NV, 2007.

16. TPI Composites, “Innovative Design Approaches for Large Wind Turbine Blades; Final Report,” SAND2004-0074, Sandia National Laboratories, Albuquerque, NM.
17. Griffin, D. A., “Blade System Design Studies Volume II: Preliminary Blade Designs and Recommended Test Matrix,” SAND2004-0073, Sandia National Laboratories, Albuquerque, NM, June 2004.
18. Berry, D., “Design of 9-Meter Carbon-Fiberglass Prototype Blades: CX-100 and TX-100,” SAND2007-0201, Sandia National Laboratories, Albuquerque, NM, September 2007.
19. TPI Composites, Inc., “Blade Manufacturing Improvements Development of the ERS-100 Blade,” SAND2001-1381, May 2001.
20. Paquette, J.P. and Veers, P.S., “Increased Rotor Size through Passive Load Control and Weight Reduction Concepts,” *EWEC 2009*, March 2009.
21. Ashwill, T.D., Kanaby, G., Jackson, K., Zuteck, M. D., “Development of the Sweep-Twist Adaptive Rotor (STAR) Blade,” *48th AIAA Aerospace Sciences Meeting*, Orlando, FL, January 2010.
22. Knight & Carver Wind Group, “Sweep-Twist Adaptive Rotor Blade: Final Project Report,” SAND2009-8037, Sandia National Laboratories, February 2010.